Highlights of Spanish Astrophysics XI, Proceedings of the XV Scientific Meeting of the Spanish Astronomical Society held on September 4–9, 2022, in La Laguna, Spain. M. Manteiga, L. Bellot, P. Benavidez, A. de Lorenzo-Cáceres, M. A. Fuente, M. J. Martínez, M. Vázquez- Acosta, C. Dafonte (eds.), 2023

EMIR upgrade: installing a new Hawaii 2RG detector.

Garzón, F.[1,2], **Joven, E.**[1,2], **Rodríguez, H.**[1,2], **and Mato, Á.**[1,2] **and Rosich, J.**[1,2]

[1] Instituto de Astrofísica de Canarias, IAC, Vía Láctea s/n, 38205, La Laguna (S.C. Tenerife), Spain
[2] Departamento de Astrofísica, Universidad de La Laguna, 38206, La Laguna (S.C. Tenerife), Spain

Abstract

EMIR is one of the first common user instruments for the GTC, the 10 meter telescope operating at the Roque de los Muchachos Observatory (La Palma, Canary Islands, Spain). EMIR has been built by a Consortium of Spanish and French institutes led by the Instituto de Astrofísica de Canarias (IAC). The instrument is primarily designed to be operated as a MOS in the K band, but offers a wide range of observing modes, including imaging and spectroscopy, both long slit and multi-object, in the wavelength range 0.9 to 2.5 μm.
EMIR had its first light on June 2016 and started routine observation in 2017, while the MOS mode was commissioned and offered to the community in 2018. Since the beginning, EMIR performances were hampered by the high noise and instabilities of its detector, a Hawaii2 2048^2 array. We had no option but to use this low quality item as the original detector, much superior in virtually every aspect, was flagged with potential risk of explosion due to a defect in the fabrication procedure, that was corrected in subsequent fabrication batches. At that time, there were no more detectors available of the same type, a PACE architecture in the hybrid Silicon chip plus MCT. The lack of sensitivity due to the signal instabilities is more pronounced in spectroscopic mode, while the data frames taken in image mode could be cleaned to a large extent.
With support from the Spanish national funding agency, GRANTECAN has acquired two Teledyne Hawaii2 RG + ASIC to be used in the EMIR and FRIDA instruments. We are characterising the arrays in the lab and are executing a complex plan to permit the replacement of the EMIR detector in short time. This plan includes changes in the control software and a new detector assembly with piezoelectric actuators for remote control and adjustment of the alignment.
In this contribution we will provide a short description of the main problems of the current detector and will show how the new detector will improve significantly in all of these. We will also mention the current plans for installation.

1 Introduction

Among the large instrumental suite in each of these new telescope stations, multi-object spectrographs (MOS) play a prominent role and are always in the top rank of the most demanded

instruments. The near-infrared (NIR) MOS is particularly interesting for large telescopes as the NIR permits the detection of objects in the optical bands hidden by massive material clouds, and because of the effect of redshift in objects at cosmological distances. Given the next and upcoming generation of ground- and space-based observatories (e.g. JWST, E-ELT), NIR spectroscopy is of increasing importance. To support 30m class telescopes, well-established NIR spectrographs on 8–10m class telescopes are a vital resource, and are scientifically viable in their own right. EMIR ([4, 5, 6, 2, 3]) is occupying this niche at the Gran Telescopio Canarias (GTC).

EMIR is a NIR wide-field spectrograph, similar to other instruments developed in the 2000s for 10m class telescopes, such as KMOS/VLT[1], MOSFIRE/Keck[2], and Flamingos2/GEMINI[3]. The concept of the instrument corresponds to a classical camera and spectrograph design, but with several novelties. Its spectral working range is dictated by the spectral response of the detector, hence it spans from 0.9 to 2.5 μm. From the beginning the top priority mode of EMIR was set as multi-object spectroscopy in the K band, due to the requirements of the instrument main scientific driver, the Galaxy Origins and Young Assembly (GOYA) Survey ([7], [1]). This imposed a fully cryogenic layout of the instrument that, in addition, set a severe restriction for the multi-object capability of EMIR.

It is one of the common user instruments at the GTC, and offers observing capabilities in imaging and spectroscopy in both long-slit and multi-object modes, over a field of view of $6.67 arcmin \times 6.67 arcmin$ in image mode and $6.67 arcmin \times 6.67 arcmin$ in spectroscopy. It had its first light at the GTC in mid-2016 and was initially offered to the community in late 2017 after a long period of commissioning and science verification phases. The control system of EMIR was constantly tuned during the first years to permit a smooth coordination with the telescope and proper functioning of the different observing modes. EMIR was tested in the lab with a Hawaii2 FPA detector of the initial architecture, but we were forced to replace it, rather close to the shipping date to the GTC, due to the high risk of explosion that had happened in other similar arrays. The new detector, while free from the risk of explosion thanks to the new manufacturing process, was less adequate than the original one, due to higher read-out noise and instabilities in the signal. All together, these features led to an overall instrument performance below what was expected, in particular for faint sources. This unforeseen problem forced the instrument team to devote substantial efforts to try to alleviate the lower effective sensitivity. While in image mode we developed methods to clean the frame with remarkable success, in spectroscopy only minor improvements were achieved despite the many attempts using different approaches. It should be noted that this caveat is of particular importance, but only for faint objects. Finally, new funds arrived that permit the replacement of the detector by a new Hawaii2RG, which is currently being tested at the IAC. In the rest of the paper, we will describe the main problems observed in the current detector, will compare the performances of the two slates as they have been measured so far, and will summarise the status of the replacement project and expected schedule.

[1] http://www.eso.org/public/teles-instr/paranal-observatory/vlt/vlt-instr/kmos
[2] https://www2.keck.hawaii.edu/inst/mosfire/home.html
[3] https://www.gemini.edu/instrumentation/flamingos-2

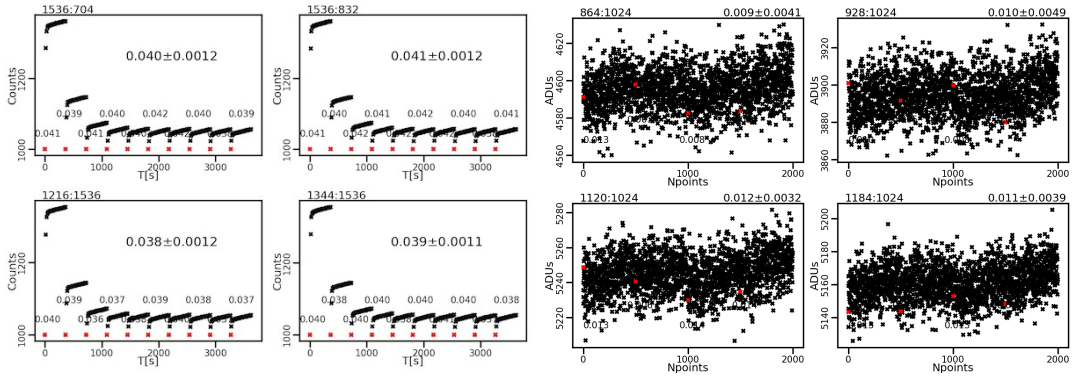

Figure 1: DC measurement test where ramps were taken with the instrument was fully closed to avoid any illumination onto the detector. Left panel: 4 channels of the current detector, with 10 ramps. Right panel: same test, but with the new detector mounted in the testing cryostat at the IAC, and with 4 ramps in total. See text for details.

2 The problem with the current detector

As it has been mentioned above, during the AIV phase of the EMIR instrument at the IAC, we had to replace the detector array, mounted on EMIR during a large fraction of the testing phases, for a new one due to the reasons already mentioned. Since the beginning, this new array exhibited an abnormal behaviour, particularly marked at low signal levels. Needles to say that the target objects at the faintest possible limit are of utmost interest for the observing programmes in 10 m class telescopes as the GTC.

Figure 1-left shows an example of the main caveat in the performances of the current EMIR detector. This is the result of a Dark Current (DC) test. During this measurement, the instrument was closed to the maximum possible extent – external window, CSU, grism and filter wheels in closed positions – to ensure complete darkness inside the cryostat. Then, the detector registers the signal produced by itself, that is called dark current. This current sets typically the sensitivity limit of the detector, together with the read-out noise (RON). In fig. 1 , each panel shows the result of one of the 4 central panel out of the 32 readout channel of the detector, as its architecture permits the simultaneous read through 32 separated channels, each one in charge of a subset of the full detector pixel set, hence diminishing the readout time by a factor of 32. On each panel, the average signal of the central 5000 pixels of each subset is marked as a single point in black. The red points correspond to the initial read of each ramp that are followed by 27 reads, totalling 28 non-destructive reads on each ramp in the left panels. 10 ramps were taken on this test. Each panel shows the trend of the 10 ramps in counts vs. time from the start of the test. The ramps were taken without any time shift in between them, as in the routine measurements on sky objects. What is of interest for the user is the slope of the ramp, from which the incident flux can be derived after proper calibration.

Two main features can be seen in fig. 1-left. At first, there is a clear shoulder on the

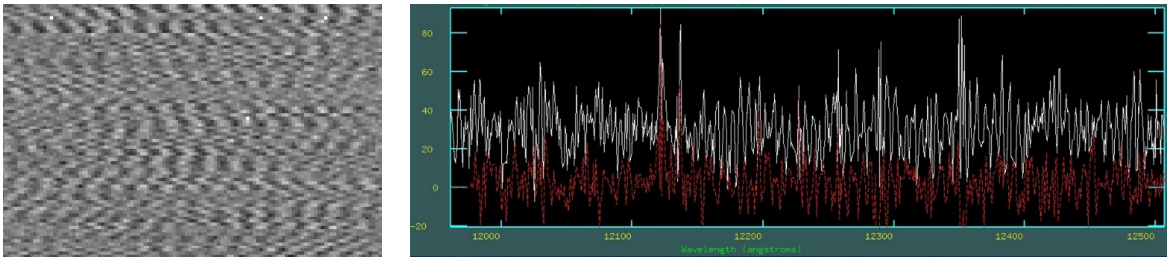

Figure 2: Left panel: detail of an area of the detector free of target signal during an observation. Right panel: portion of an object spectrum without cleaning, in white, and after cleaning, in red.

ramps, with the first 3–4 points climbing much steeper than the rest of the ramps. This effect is mostly due to a parasitic signal in the detector, that is added to signal produced by the target object. As a result, the first points cannot be used to derive the slope of the ramp, hence this calculation has to be performed with a smaller set of points than the total number of reads, that yields a poorer signal to noise ratio. The numbers close to each individual ramp are the slopes calculated using only the second half of the read points. And the numbers in the middle of each panel represent the average of the 10 measurements plus the standard deviation. The second issue is the fact the the first ramps behaves differently than the last ones. Depending upon the incident flux, which in this test is virtually null, there are a number of ramps that show a more pronounced shoulder than the rest of the series. In fig. 1-left, the first 3–4 ramps show this effect. Fortunately, the second half of this abnormal ramps are aligned with the rest of the set, so they can be used in the calculations. A third issue that is not visible in fig. 1-left consists in marked jumps in the reset level, that sets the initial level for the integration. Figure 1-left has all these pedestal level, marked in red, arbitrarily set to 1000 adu, hence displacing vertically each ramp a different amount. Without this artificial manipulation, that does not change the slopes, the comparative analysis of the ramps would have been a bit more difficult, as these jumps are of the order of a few hundred counts.

The above described effects are associated to intrinsic currents within the detector and to the reading procedure. So it is not unexpected that they show as a correlated pattern in the read frame. Figure 2 shows this pattern in a section of the frame free of spectral lines that would otherwise make more difficult to see the *regularity* of the pattern. We have taken advantage of this similarity to design cleaning procedures that works until a given extent, as can be seen in the right panel of fig. 2. The reduction in the spectrum noise in this case is a factor of 3. Regrettably, the cleaning fails in the presence of abundant sky lines, as in the H and K spectral bands, as there is no section of the detector frame free of input flux of sufficient extent to derive the pattern noise.

All in all, plus other less important features that are not commented in this paper, result of an irregular and unstable behaviour of the detector, which a clear impact in the performances of the whole instrument so, after receiving additional funds, we are now in the process of replacing the current detector for a new model of a modern and different technology and free of these flaws.

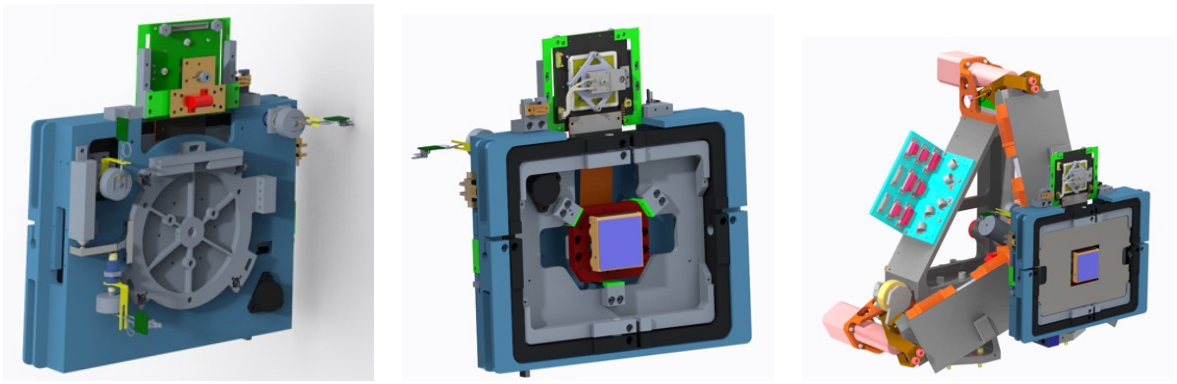

Figure 3: Several views of the design of the new detector mount. The green card on top the mount represent the ASIC unit of the new detector, that takes care of much of the detector driving. The right panel shows the complete set detector plus mount assembled onto the EMIR DTU.

3 New detector: short summary of performances and current installation plans

GRANTECAN received funds from the national agency to purchase two complete sets of detector array Hawaii2RG, which are currently been tested at the IAC. The item that will replace the EMIR detector is now fully tested in lab, and its performances, as far as DC is concerned, can be compared with that the current one in fig. 1. The right panel shows the DC measurements of 4 channels, with the same color code as in the left panel explained in Section 2, but with 500 reads on each ramp. In this case, the ramp points are depicted without correction for pedestal level. It can be seen that the red points aligned within a few counts, and that there is no shoulder in the ramps, that are mostly pure noise, as it should be. Also the average DC levels, showed on top of each panel in the right side of fig. 1, are much smaller than in the left side. And additional good feature of this new array resides on its flatness, that has been measured to be as small as 11μm peak-to-valley, that has to be compared with the figure of around 100μm in the current detector, that should result in a better image quality once mounted in EMIR. In addition, the new detector will be seated in a new gimbal mount, see fig. 3, equipped with remote controlled piezo-electric actuators to permit an fine tilt alignment once integrated onto the instrument.

At this time, we are finalising the construction of the new mount that will be assembled and tested in the next months. Also, the engineering team is updating the EMIR control software to cope with the driving of new detector, which is now controlled through a dedicated SIDECAR ASIC provided by the detector vendor.

We are expecting to be able to initiate tests on sky, with the new detector mounted in EMIR, during the first semester of 2023, but this tentative schedule has to be put in context with GRANTECAN and IAC capabilities and availabilities.

Acknowledgments

EMIR has been funded by GRANTECAN S.L. via a procurement contract; by the Spanish funding agency grants AYA2001-1656, AYA2002-10256-E, FIT-020100-2003-587, AYA2003-01186, AYA2006-15698-C02-01, AYA2009-06972, AYA2012-33211, AYA2015-63650-P, AYA2015-70498-C2-1-R and PGC2018-102249-B-I00; and by the Canarian funding agency grant ACIISI-PI 2008/226.

References

[1] Balcells, M. 2003, Revista Mexicana de Astronomía y Astrofísica Conference Series, 16, 69-72

[2] Garzón, F., 2016, Astronomical Society of the Pacific Conference Series, 507, 297

[3] Garzón, F., Abreu, D., Barrera, S., Becerril, S., Cairós, L. M., Díaz, J. J., Fragoso, A. B., Gago, F., Grange, R., González, C., López, P., Patrón, J., Pérez, J., Rasilla, J. L., Redondo, P., Restrepo, R., Saavedra, P., Sánchez, V., Tenegi, F. & Vallbé, M. . 2006, SPIE, 6269, 626918

[4] Garzón, F., Balcells, M., Gallego, J., Gry, C., Guzmán, R., Hammersley, P., Herrero, A., Muñoz-Tuñón, C., Pelló, R., Prieto, M., Bourrec, É., Cabello, C., Cardiel, N., ez, C., Laporte, N., Milliard, B., Pascual, S., Patrick, L. R., Patrón, J., Ramírez-Alegría, S. & Streblyanska, A. . 2022, A&A, 667, A107

[5] Garzón, F., Castro, N., Insausti, M., Manjavacas, E., Miluzzio, M., Hammersley, P., Cardiel, N., Pascual, S., ez, C., Molgó, J., Barreto, M., ez, P., Joven, E., López, P., Mato, A., Moreno, H., Núnez, M., Patrón, J., Rosich, J. & Vega, N. . 2017, Highlights on Spanish Astrophysics IX, 652-659

[6] Garzón, F., Castro, N., Insausti, M., Manjavacas, E., Miluzio, M., Hammersley, Peter, Cardiel, N., Pascual, S., ez, C., Molgó, J., Barreto, M., ez, P., Joven, E., López, P., Mato, A., Moreno, H., Núñez, M., Patrón, J., Rosich, J. & Vega, N. . 2016, SPIE, 9908, 99081J

[7] Guzmán, R.2003, Revista Mexicana de Astronomía y Astrofísica Conference Series, 16, 209-212